Jour. of the KGS, Vol. 23, No. 9. September 2007, pp. 29~37

A Simple Model of Shrinkage Cracking Development for Kaolinite

수축 균열 발달 과정을 위한 단순 모델

Min, Tuk-Ki[1] 민 덕 기

Vo Dai Nhat[2] 보 다이 낫

요 지

본 연구에서는 카올린점토에 대한 실내실험을 통하여 수축으로 인한 균열발생을 조사하고 균열 단계를 모사할 수 있는 단순모델을 제안하였다. CPS 기법을 이용하여 디지털 카메라에 의해 얻은 균열 이미지를 분석하였다. 함수비의 감소에 따라 균열의 길이와 면적은 1차 균열단계, 2차 균열단계, 수축단계 균열의 3단계로 나타났다. 균열 면적의 1차 및 2차 균열 최종 단계에서의 정규화된 함수비는 시료 두께에 상관없이 각각 0.92와 0.70에서 발생하였다. 반면 균열 길이는 1차 균열 최종 단계에서의 함수비는 시료 두께와 상관없이 0.92에서 발생하였으나, 2차 균열 최종 단계에서의 함수비는 시료 두께가 0.5, 1.0, 2.0cm로 증가함에 따라 함수비는 0.79, 0.82, 0.85로 증가하였다. 수축 균열을 모사할 수 있는 3개의 직선으로 구성된 단순모델을 제안하였다.

Abstract

The experiments have been conducted on Kaolinite in laboratory to investigate the development of shrinkage cracking and propose a simple model. Image analysis method consisting of control point selection (CPS) technique is used to process and analyze images of soil cracking captured by a digital camera. The distributions of crack length increment and crack area increment vary as a three-step process. These steps are regarded as stages of soil cracking. They are in turn primary crack, secondary crack and shrinkage crack stages. In case of crack area, the primary and secondary stages end at normalized gravimetric water content (NGWC) of 0.92 and 0.70 for different specimen thicknesses respectively. In addition, the primary stage in case of crack length also ends at NGWC of 0.92 while the secondary stage stops at NGWC of 0.79, 0.82, and 0.85 for the sample thicknesses of 0.5, 1.0, and 2.0 cm respectively. Based on the experimental results, the distributions of crack length increment and crack area increment appear to be linear with a decrease of NGWC. Therefore, the development of shrinkage cracking is proposed typically by a simple model functioned by a combination of three linear expressions.

Keywords : CPS, Crack area increment, Crack length increment, DIP, Kaolinite, NGWC, Shrinkage cracking

1. Introduction

Generally, soil cracking is a natural phenomenon and frequently observed in many natural and man-made structures such as buildings, dams, etc. Cracking in soils due to drying is controlled by partly soil suctions and partly soil properties including mainly the physical and the chemical properties. Solutions for cracking due to drying have been introduced and developed based on (i) elasticity theory, (ii) the transition between tensile and shear failure, and

1 Member, Prof. Dept. of Civil & Environ. Engrg., Univ. of Ulsan, tkmin@ulsan.ac.kr, Corresponding Author

2 Researcher, Dept. of Civil & Environ. Engrg., Univ. of Ulsan, nhatvodai@yahoo.com

(iii) linear elastic fracture mechanics (Morris et al., 1993). Cracks appear when soils are restrained while undergoing volume change produced as a result of the soil suction generated within the desiccating soil matrix. A review of the available and emerging theories of desiccation cracking of clay containing some laboratory tests has been presented (Kodikara et al., 2000). The results showed that cracking of clay generally depends on experiment conditions such as base material, soil density, the desiccation rate, and thickness of the sample. Conditions that govern the characteristics of soil cracking may be categorized as two separate terms: extrinsic and intrinsic conditions (Wijeyesekera and Papadopoulou, 2001). Extrinsic conditions include fundamentally the temperature, relative humidity, and wind velocity whereas moisture condition, structure of material, degree of packing, physical and chemical composition, etc belong to intrinsic conditions. In addition, cracking formation also can be affected by the microbial contribution (Preston et al., 2001). These effects were assessed by quantifying the heterogeneity and connectivity of cracks developed following the addition of substrate differing in quantity and quality to a sandy loam soil. Furthermore, the characteristic of relationships between water content, bulk density, and cracking was also investigated by Waller and Wallender (1993). Many physical investigations of the cracking have been published with various materials conditions such as Homand et al. (2000), Konrad and Ayad (1997), Karmakar et al. (2005) and Velde (1999).

To implement the understanding of the cracking of soil, theoretical and numerical studies of desiccation of soil have been investigated by employing linear theories of hygro-elasticity and moisture diffusion for rectangular slabs (Hu et al., 2006). There have been some experimental works on desiccation cracks such as effect of desiccation on compacted natural clays (Albrecht and Benson, 2001) and desiccation and cracking behavior of three compacted landfill liner soils (Yesiller et al., 2000). Basically, the geometry of soil cracks including surface crack area and surface crack length plays an important role in water flow. The possible measures can be done using digitized images to quantify soil structure (Velde, 2001; Peng et al., 2006 and Vogel et al., 2005). Theoretical studies have been made of cracks based on analyzing in detail crack-surface morphology of the nucleation and growth path of natural mud (Weinberger, 1999).

The development of soil cracking has been known as a complex process consisting of stages. An initial step in understanding the development of soil cracking is the study of crack growth formed by shrinking at the surface of the soil due to drying. This study is conducted to investigate the development of shrinkage cracking of Kaolinitic soil. The amount of cracking on the surface of the soil – crack length and crack area – is quantified using image analysis method and computed automatically by using Matlab program. To reduce the errors, an application of CPS technique is applied. Then the distributions of crack length and crack area increment with NGWC are established. They are proposed approximately by a simple model functioned by a combination of three linear expressions. Finally, the typical shape of shrinkage cracking development is presented experimentally.

2. Fundamental of Evaporation and Shrinkage Cracking

2.1 Evaporation

Evaporation appears from the soil surface. Consequently, the mass of the soil system will decrease by a loss of water. This leads to a decrease of gravimetric water content of the system. The evaporation rate is affected by conditions such as temperature, relative humidity, and wind velocity, etc. The flux of soil water upward to the soil surface is dominated by the hydraulic properties of the soil such as unsaturated hydraulic conductivity, water potential gradient, and thermal gradient in soil. The evaporation rate computed from the water loss is determined totally by both the external conditions and the internal properties of the soil system.

2.2 Shrinkage Cracking in Drying Soils

Shrinkage cracking is one of the most common types of cracking found in the earth structures. As water is lost

from the surface soil mass, tensile forces are established in the drying surface layer and soil also loses its ability to relieve these tensile forces. These stresses are finally relieved by the occurrence of cracks that grow up at the surface of the soil. The natural formation of soil structure is always related to the water loss and the characteristic of shrinkage cracking in drying soils.

In drying soils, the soil particles move closer and closer together. If the drying proceeds from the surface downward, then the surface layer shrinks while the water resistance between the upper and lower layers and in the layers themselves prevents an adjustment to the volume decrease of the surface layer. Consequently, tensile stresses causing the creation of cracks are developed in the surface layer. When the soil is restrained in some ways against shrinkage, desiccating clay tends to crack as the tensile stress which is developed in the soil because the matric soil suction exceeds the tensile strength of the soil. The restraints can be external (layer interfaces, boundary conditions, and the shape of the border) and/or internal (non-uniform drying in soil layers).

3. Preparation of Sample

The experiment was performed in a steel rectangular tray. Firstly, the soil was mixed carefully with water and stirred in a stirrer for half an hour to constitute a paste. An initial water content of the mixture was about 65%, 1.5 times higher than liquid limit. Liquid limit, plastic limit, and plasticity index of the studied soil are 42.07, 25.40 and 16.67% respectively. Secondly, the mixture was poured in the tray and uniformly spread to make the surface flat. Finally, the system was balanced and allowed to dry naturally in laboratory at room temperature $22\pm4^{0}C$ and humidity of 50-60%. Thickness of the specimen was varied with three sets of 0.5, 1.0, and 2.0 cm. The drying process has continued for several following days. The specimen was kept in a close watch to observe accurately when cracks initiate.

4. Digital Image Processing (DIP)

4.1 Image Capture

Images of the specimen were captured by a digital camera (Olympus C-5050 zoom). To unify totally testing conditions, two 300-W halogen lamps were used and positioned at fixed location. Additionally, the camera's position was fixed to capture the whole region of the specimen. Together with capturing the images of soil cracking, the mass of the soil system was measured simultaneously in order to calculate the correspondingly gravimetric water content.

4.2 Image Processing

To reduce the errors which can occur in using DIP, CPS technique might be used. The procedure of CPS technique can be summarized generally in Figure 1.

Firstly, the base image and the unregistered image were read automatically. To use CPS technique, the base image (Figure 2a) including the base points and the input image with the selected input points are required compulsorily. The base points are considered as four points near the corners. Figure 2b shows an example of the unregistered image consisting of the four input points locating at the top of arrows. One should note that the base points and the input points are selected manually; hence, the selection must be done carefully.

Secondly, in order to transform the unregistered image, a type of transformation was required to transform the unregistered image based on the input points and the base

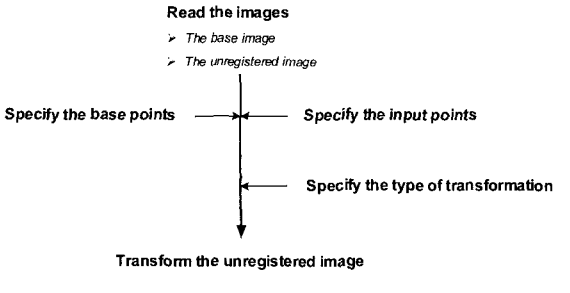

Fig. 1. Illustration of CPS procedure

points. The transformed image resulted from the base image (Figure 2a) and the unregistered image (Figure 2b) was presented in Figure 2c. In order to eliminate the effects of the border, the image was cropped to obtain the properly inside region.

Finally, the expected image was resized as a dimension of 1280x960 pixels as shown in Figure 2d corresponding to the real size of the tray 220 mm by 165 mm. To perform quantitative measurements in the image, the finally expected image was converted to binary image.

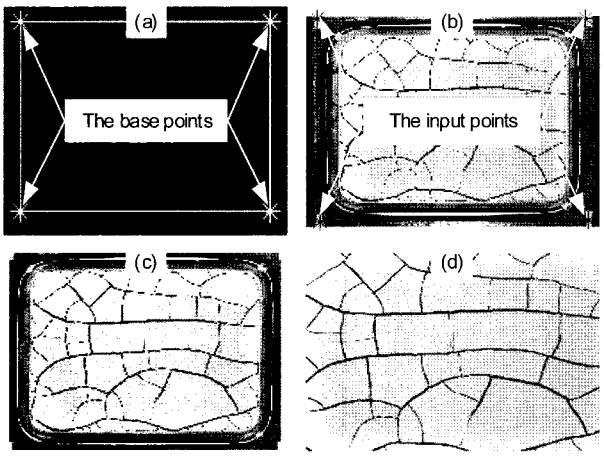

Fig. 2. Transformation of the unregistered image: (a) the base image and points, (b) the unregistered image and the input points, (c) the transformed image, and (d) the finally expected image

Examples of binary images of cracks developing with an increase of drying time are presented in Figure 3. Four images on the top row are of 0.5 cm, the middle of 1.0 cm, and the bottom of 2.0 cm in thickness respectively. In each row, the first image is an initial image. The two following images are the developed cracking images as drying time increases. And the last one is considered as the final image for the development of shrinkage cracking.

4.3 Measurement of Crack Length and Crack Area

For quantitative measurements, binary images of cracking were used to compute automatically by using Matlab program. The two principal parameters of the generated cracks were analyzed: length and area. Cracks are occupied by black pixels while white pixels are considered as the background.

Crack area was computed automatically by counting the total number of black pixels as shown in Figure 4a. To measure crack length, the color of cracks is required to be converted from black to white (Figure 4b) for applying an algorithm 'thin' defaulted in the program. The command

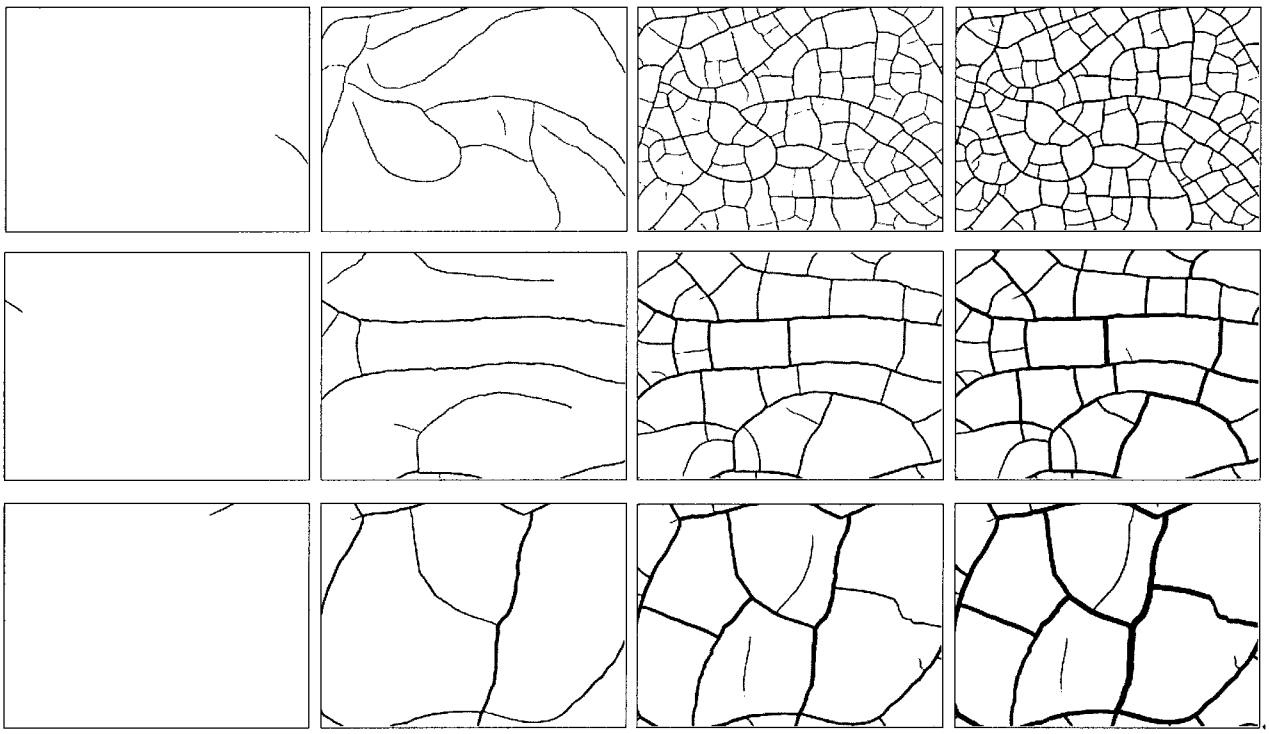

Fig. 3. Examples of binary images developing with drying time for thicknesses: the first row 0.5 cm, the second row 1.0 cm, and the third row 2.0 cm, respectively

'bwmorph' was used to calculate crack length with 'thin' option. Using this algorithm, cracks were thinned to lines automatically as presented in Figure 4c. Crack length was calculated by a sum of distances of continuously consecutive pixels from Figure 4c.

5. Experimental Results

5.1 Crack Length

Parallel to capturing image of soil cracking, the mass of the soil system was measured simultaneously to calculate gravimetric water content. With an increase of drying time, the mass of the system will decrease continuously due to a loss of water. When water content of the system reaches a critical value, cracks initiate. In this study, the experimental results show that cracks initiate at gravimetric water content of about liquid limit. This value is denoted W_0.

Figure 5 presents the variation of crack length L with NGWC. The measured data are plotted by solid points for the cases of the specimen thickness. At first, crack length increases continuously with a decrease of NGWC. It, then, achieves a constant value and becomes clearly unchangeable. With larger thickness, it increases slower and the constant of crack length is smaller. They are experimentally 4500, 2200, and 1300 mm for the specimen of 0.5, 1.0, and 2.0 cm in thickness respectively. Furthermore, these constants are obtained at different values of NGWC for different specimen thicknesses. The larger the specimen thickness, the higher the NGWC is. Experimentally, they are about 0.79, 0.82, and 0.85 for the specimen thicknesses of 0.5, 1.0, and 2.0 cm respectively.

5.2 Crack Area

As a result of crack growth, an increase of crack results in an increase of crack area. Similar to the variation of crack length, crack area increases as gravimetric water content decreases. The variations of crack area A with NGWC for different thicknesses are given in Figure 6.

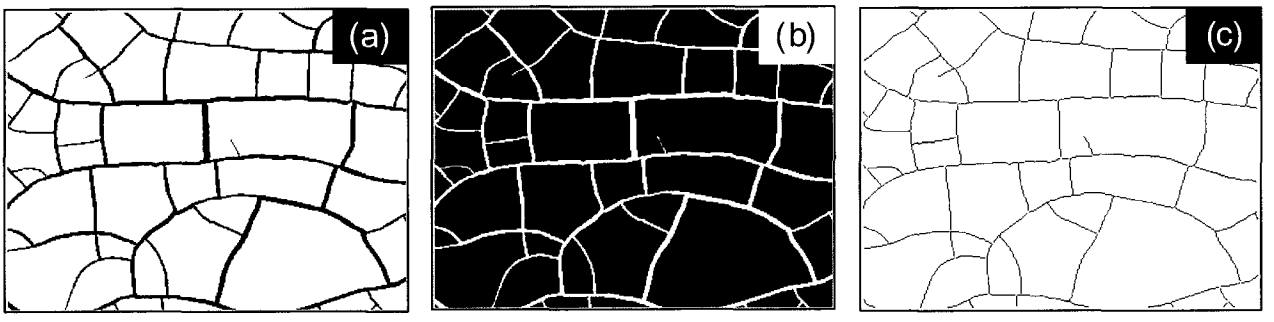

Fig. 4. Images for calculating crack area and crack length: (a) crack area, (b) converted image, and (c) crack length.

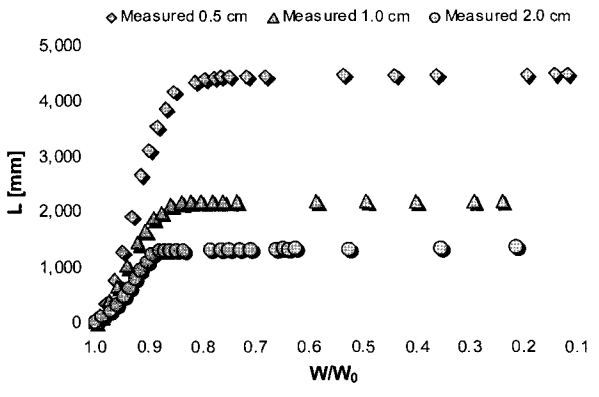

Fig. 5. Variation of crack length with NGWC for different specimen thicknesses

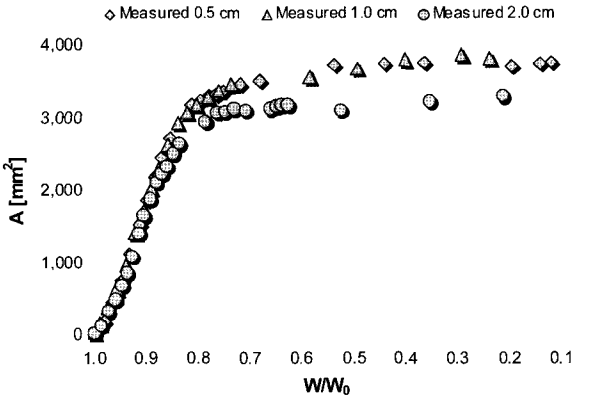

Fig. 6. Variation of crack area with NGWC for different specimen thicknesses

As shown in Figure 6, the same as an increase of crack length, crack area increases continuously from NGWC of 1.0 to reach a constant value and becomes unchangeable. In contrast to an increase of crack length, crack area appears to be the same for the cases of the specimen thickness in a range of NGWC. Hence, it is expected that crack area can be the same for the cases of the specimen thickness in this study. However, as NGWC continues decreasing crack area only appears to be the same in two cases of the specimen thickness of 0.5 and 1.0 cm. In case of 2.0 cm in thickness, crack area is smaller than in the others. That can be explained by a lack of a few cracks from the selection of the proper image region by eliminating a few cracks appearing along the border of the container. In addition, that can also be explained by considering the non- uniformity of the specimen as the specimen thickness becomes larger.

6. Modeling

6.1 Crack Length as a Function of Gravimetric Water Content

Modeling is one of the challenges for describing the development of shrinkage cracking because it is a complex process consisting of stages. In order to understand fully the development of shrinkage cracking, increment of crack length is calculated by the deviation of crack length to NGWC. The distribution of crack length increment is illustrated by solid points in Figure 7. As can be seen, it firstly increases to achieve a peak; secondly, it decreases to zero; and finally, it becomes unchangeable with zero value.

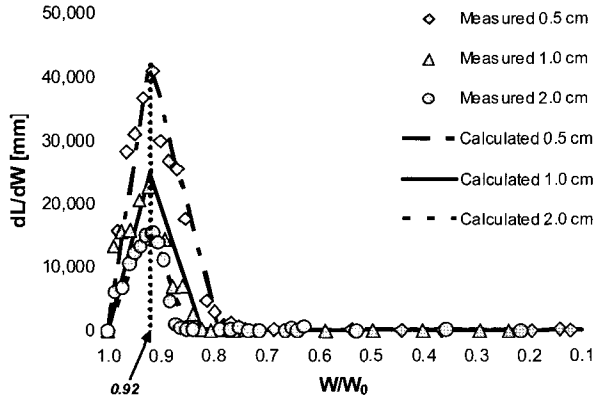

Fig. 7. The distribution of crack length increment with NGWC (solid points are the experimental data; the continuous lines are calculated from the proposed simple model)

Increment of crack length reaches a peak at NGWC of 0.92 (as given in Figure 7, denoted by the dot line) for three cases of the specimen thickness. However, as the thickness increases, the peak value decreases. Due to the effects of the specimen thickness, the constant zero values of crack length increment are obtained at different values of NGWC. The larger the specimen thickness is given the higher the value of NGWC becomes. These are experimentally 0.79, 0.82, and 0.85 for the specimens of 0.5, 1.0, and 2.0 cm in thickness respectively. With smaller thickness, crack length increment increases to achieve a peak and then decreases to reach a value of zero more quickly.

It appears generally that the distribution of crack length increment varies linearly with NGWC for each step. Therefore, an attempt has been carried out for simplifying the distribution of crack length increment. Each step is modeled by a linear expression. Consequently, the distribution of crack length increment is described by a combination of three linear expressions as illustrated in Figure 7 by the continuous lines. Based on the experimental results, the proposed model starts at NGWC of 1.0. It increases linearly to achieve a peak at NGWC of 0.92. Then it decreases linearly to zero at NGWC of 0.79, 0.82, and 0.85 for the specimen thicknesses of 0.5, 1.0, and 2.0 cm respectively. Finally, it becomes unchangeable with value of zero. As can be seen in Figure 7, the measured data (solid points) and the calculated values (lines) determined by the proposed simple model demonstrate an acceptable appearance.

6.2 Crack Area as a Function of Gravimetric Water Content

Similar to the distribution of crack length increment, crack area increment was calculated as a deviation of crack area to NGWC. The distribution of crack area increment (shown in Figure 8 by solid points) obeys a

three-step process which is the same as the distribution of crack length increment. It firstly varies increasingly to achieve a peak; secondly, it varies decreasingly to zero; and finally, it becomes unchangeable with zero value. Increment of crack area reaches a peak at NGWC of 0.92 denoted by the dot line for three cases of the sample thickness, the same as that in case of crack length. However, the peak seems to be same for different thicknesses. Subsequently, the second step ends at NGWC of 0.70 for three cases of the specimen thickness as shown in Figure 8.

Each step of crack area increment appears experimentally to be linear with NGWC. Hence, a combination of three linear functions is used to model the distribution of crack area increment. The proposed model is superimposed in Figure 8 by the continuous line. The first step starts at NGWC of 1.0 and ends at that of 0.92. The second step varies from NGWC of 0.92 to that of 0.70 for three cases of the specimen thickness. The experimental data and the predicted values give an acceptable appearance.

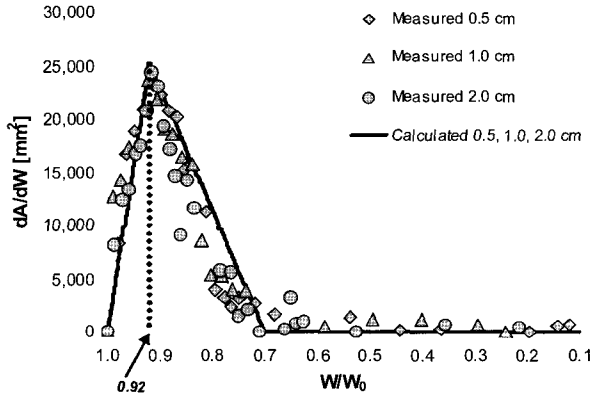

Fig. 8. The distribution of crack area increment with NGWC (solid points are the experimental data; the continuous line is calculated from the proposed simple model)

7. Discussion

The object of this study is to analyze and propose a simple model for the development of shrinkage cracking in unsaturated Kaolinitic soil due to drying based on the distributions of crack length and crack area increments with NGWC. The study uses image analysis method consisting of CPS technique to quantify length and area of cracks in Kaolinite.

With an application of CPS technique, the errors which can be caused by movement of camera due to capturing images will be reduced considerably. However, one should note that the selection of control points, the base points and the input points, is made manually; hence, this process must be done carefully. By observing the specimen hourly, the experimental results are sufficiently reliable. As shown in Figure 4, the first images in three rows are the initial images captured when cracks initiate.

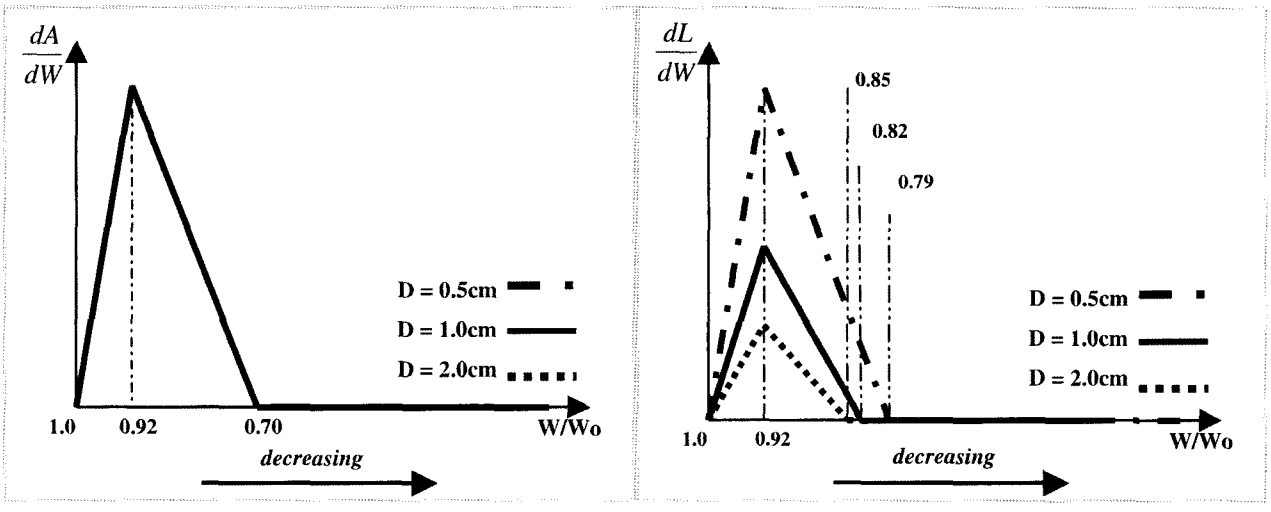

Fig. 9. Typical distribution shapes for the development of shrinkage cracking in unsaturated Kaolinitic soil in terms of increment of crack area, *dA/dW* (left-hand) and crack length, *dL/dW* (right-hand) as a function of normalized gravimetric water content *W/W*$_o$. The numbers in Figure are only for Kaolinite experimentally.

It was found that the distributions of crack length and area increments obey a three-step process: (1) increase linearly to achieve a peak; (2) vary decreasingly to zero; and finally (3) become unchangeable with value of zero. This process corresponds to three stages of cracking in soils: primary crack stage, secondary crack stage and shrinkage crack stage respectively. These steps appear to be linear. Consequently, each stage is simplified by a linear function. The proposed simple models are presented schematically in Figure 9. The numbers on Figure 9 illustrate experimentally only for Kaolinite. This model can help us in understanding crack growth and in interpreting the patterns seen in the soil. In general, it is obvious that many functions can be used to model the development of shrinkage cracking in soil described through the distribution of crack (length and area) increment. However, the dominant advantage of a linear function is simple for use and application. Furthermore, the calculated values and the experimental results appear acceptably.

In addition, there are effects of the specimen thickness on gravimetric water content, crack length, and crack area. They result in the effects of the specimen thickness on stages of the distributions of crack length and area increments. In case of crack area increment, the same peak value is achieved experimentally at NGWC of 0.92 and the end of the second stage finishes completely at NGWC of 0.70 for three cases of the specimen thickness. However, there are differences in case of crack length. The peak value of increment of crack length is achieved at the same value of NGWC of 0.92, but as thickness increases the peak value decreases. Furthermore, the second stage finishes completely at different values of NGWC. With smaller thickness, the value of NGWC at the end of the second stage is smaller. Experimentally, they are 0.79, 0.82, and 0.85 in cases of the sample thicknesses of 0.5, 1.0, and 2.0 cm respectively. The different gravimetric water contents due to different thicknesses can be explained by the variation of water content with depth as considered in reference 7. If the specimen thickness is considered as a combination of thin layers, the average water content of each layer will increase with depth from the soil surface. In this study, gravimetric water content was calculated averagely for the system while cracks initiate and develop from the surface of the soil mass. Therefore the second stage ends at higher value of NGWC with larger thickness specimen.

Beside the effects of the specimen thickness, experiment conditions such as temperature, relative humidity, wind velocity, non-uniform drying, and image analysis also can affect the results. This is proved through the fluctuation of the experimental data plotted on the graphs, especially in case of crack area. Due to shrinkage of cracks, the variation of crack length is observed more clearly than that of crack area. However, the distribution of crack length increment describes the second stage of cracking better while the distribution of crack area increment describes shrinkage stage more clearly than that of another. The effects of shrinkage of cracks are shown through the different values of NGWC at the end of the second stage between crack length and crack area. In case of crack length, NGWC at the end of the second stage is higher than that in case of crack area. Although the study has a few weak points due to the experiment conditions, a trend of the development of shrinkage cracking is observed and described clearly.

8. Conclusions

We have conducted experiments in laboratory to investigate the development of shrinkage cracking of Kaolinite due to drying naturally. Image analysis method was used to quantify crack parameters including length and area. CPS technique is applied to reduce the errors in using DIP. The development of shrinkage cracking was demonstrated through the distributions of crack length increment and crack area increment with NGWC. It was found generally that they vary as a three-step process: (1) an increasing step, (2) a decreasing step, and (3) a constant step of zero value. These steps correspond to soil cracking stages: (1) primary crack stage, (2) secondary crack stage and (3) shrinkage crack stage respectively. The development of shrinkage cracking, then, is simplified by a combination of three linear expressions. In case of crack length, the

primary stage ends at NGWC of 0.92 for three cases of the specimen thickness while the secondary stage stops at NGWC of 0.79, 0.82, and 0.85 for the specimen thicknesses of 0.5, 1.0, and 2.0 cm respectively. Different partly from crack length, the primary stage in case of crack area ends at NGWC of 0.92 but the secondary stage stops at the same NGWC of 0.70 for three cases of the specimen thickness. The experimental data and the calculated results determined by the proposed model give an acceptable appearance.

Acknowledgement

This research was supported by the 2007 Research Fund of University of Ulsan.

References

1. Albrecht, B. A. and Benson, C. H. (2001), "Effect of Desiccation on Compacted Natural Clays", *Journal of Geotechnical and Geoenvironmental Engineering*, Vol.127, No.1, pp.67-75.
2. Homand, F., Hoxha, D., Belem, T., Pons, M-N. and Hoteit, N. (2000), "Geometric Analysis of Damaged Microcracking in Granites", *Mechanics and Materials*, Vol.32, Issue.6, pp.361-376.
3. Hu, L. B., Peron, H., Hueckel, T. and Laloui, L. (2006), "Numerical and Phenomenological Study of Desiccation of Soil", *Advances in Unsaturated Soil, Seepage, and Environmental Geotechnics (GSP 148)*, Proceedings of Sessions of GeoShanghai 2006, pp.166-173.
4. Karmakar, S., Kushwaha, R.L. and Stilling, D. S. D. (2005), "Soil Failure Associated with Crack Propagation for an Agricultural Tillage Tool", *Soil and Tillage Research*, Vol.84, Issue.2, pp.119-126.
5. Kodikara, J. K., Barbour, S. L. and Fredlund, D. G. (2000), "Desiccation Cracking of Soil Layers", *Unsaturated Soils for Asia*, Rahardjo, Toll & Leong (eds). Balkema, Rotterdam, ISBN 90 5809 139 2, pp.693-698.
6. Konrad, J.-M. and Ayad, R. (1997), "Desiccation of a Sensitive Clay: Field Experimental Observations", *Canadian Geotechnical Journal*, Vol.34, No.6, pp.929-942.
7. Morris, P. H., Graham, J. and Williams, D. J. (1993), "Cracking in Drying Soils", *International Journal of Rock Mechanics and Mining Science & Geomechanics Abstracts*, Vol.30, No.2, pp.263-277.
8. Peng, X., Horn, R., Peth, S. and Smucker, A. (2006), "Quantification of Soil Shrinkage in 2D by Digital Image Processing of Soil Surface", *Soil & Tillage Research*, Vol.91, Issues.1-2, pp.173-180.
9. Preston, S., Wirth, S., Ritz, K., Griffiths, B. S. and Young, I. M. (2001), "The Role Played by Microorganisms in The Biogenesis of Soil Cracks: Importance of Substrate Quantity and Quality", *Soil Biology and Biochemistry*, Vol.33, Issues.12-13, pp.1851-1858.
10. Velde, B. (1999), "Structure of Surface Cracks in Soil and Muds", *Geoderma*, Vol.93, Issues.1-2, pp.101-124.
11. Velde, B. (2001), "Surface Cracking and Aggregate Formation Observed in a Rendzina Soil, La Touche (Vienne) France", *Geoderma*, Vol.99, Issues.3-4, pp.261-276.
12. Vogel, H.-J., Hoffmann, H. and Roth, K. (2005), "Studies of Crack Dynamics in Clay Soil I. Experimental Methods, Results, and Morphological Quantification", *Geoderma*, Vol.125, Issues.3-4, pp.203-211.
13. Waller, P. M. and Wallender, W. W. (1993), "Changes in Cracking, Water Content, and Bulk Density of Salinized Swelling Clay Field Soils", *Soil Science*, Vol.156, No.6, pp.414-423.
14. Weinberger, R. (1999), "Initiation and Growth of Cracks during Desiccation of Stratified Muddy Sediments", *Journal of Structural Geology*, Vol.21, Issue.4, pp.379-386.
15. Wijeyesekera, D. C. and Papadopoulou, M. C. (2001), "Cracking in Clays with an Image Analysis Perspective", *Clay Science for Engineering*, Adachi & Fukue (eds) Balkema, Rotterdam, ISBN 90 5809 175 9, pp.437-482.
16. Yesiller, N., Miller, C. J., Inci, G. and Yaldo, K. (2000), "Desiccation and Cracking Behavior of Three Compacted Landfill Liner Soils", *Engineering Geology*, Vol.57, Issues.1-2, pp.105-121.

(received on Jul. 13, 2007, accepted on Sep. 29, 2007)